Panoramic Structure from Motion via Geometric Relationship Detection

Satoshi Ikehata and Yasutaka Furukawa
Washington University in St. Louis

Ivaylo Boyadzhiev and Qi Shan
Zillow

Abstract

This paper addresses the problem of Structure from Motion (SfM) for indoor panoramic image streams, extremely challenging even for the state-of-the-art due to the lack of textures and minimal parallax. The key idea is the fusion of single-view and multi-view reconstruction techniques via geometric relationship detection (e.g., detecting 2D lines as coplanar in 3D). Rough geometry suffices to perform such detection, and our approach utilizes rough surface normal estimates from an image-to-normal deep network to discover geometric relationships among lines. The detected relationships provide exact geometric constraints in our line-based linear SfM formulation. A constrained linear least squares is used to reconstruct a 3D model and camera motions, followed by the bundle adjustment. We have validated our algorithm on challenging datasets, outperforming various state-of-the-art reconstruction techniques.

1. Introduction

Panorama images are everywhere on the Internet, instantly taking you to remote locations such as Rome, the Louvre, or Great Barrier Reef under water with immersive visualization. Panoramas have become the first-class visual contents in digital mapping, and are becoming increasingly more important with the emergence of Virtual Reality.

Panoramas, if equipped with the depth information, could enable 1) full stereoscopic VR experiences; 2) 3D modeling of surrounding environments; and 3) better scene understanding. However, panoramic 3D reconstruction has been a challenge for Computer Vision due to the minimal parallax, which is important to reduce stitching artifacts [24] but makes it difficult to utilize powerful multi-view reconstruction techniques. The lack of texture exacerbates the situations for indoor scenes. The reconstruction accuracy of single-view methods is still far below the production level [34, 16, 11, 28], and successful panoramic 3D reconstruction has been demonstrated only with the use of special hardware such as a depth camera (e.g., Matterport), a camera array (e.g., Google Jump), a spherical lightfield camera (e.g., Lytro Immerge), or a motorized tripod con-

Figure 1. Top: High quality panorama generation requires minimal camera translations, which make multi-view reconstruction difficult. Bottom: Our algorithm fuses single-view and multi-view reconstruction techniques to solve challenging SfM problems.

straining the motions [17].

This paper proposes a novel Structure from Motion (SfM) algorithm for indoor panoramic image streams acquired by standard smart phones or tablets (See Fig. 1). The key idea is the fusion of single-view and multi-view reconstruction techniques. In the past, 3D vision community has rarely seen such fusion, mainly because single view methods are too "rough" to be directly used with the multi-view techniques (with some exceptions [31]). We seek to utilize single-view techniques to effectively detect geometric relationships of lines (e.g., detecting 2D lines as coplanar in 3D), which in turn yield precise geometric constraints to be used in multi-view 3D reconstruction. For example, once we identify floor image regions, we can declare coplanarity among all the points or lines inside the floor regions, providing powerful geometric constraints in solving for structure and camera motions.

We formulate an SfM algorithm that expresses these geometric constraints as linear functions of our variables, and uses a constrained linear least squares to reconstruct a 3D model and camera motions, followed by the bundle adjustment. We have evaluated the proposed approach on many challenging datasets. The qualitative and quantitative evaluations have demonstrated the advantages of our method

Figure 2. Top: Subsampled input frames. While they may not look particularly difficult, the challenge lies in the minimal baseline, where standard SfM or SLAM algorithms fail. Bottom: A stitched panorama image with minimal artifacts due to the small baseline.

over many state-of-the-art reconstruction techniques.

2. Related work

This paper proposes a novel SfM algorithm that integrates single-view and multi-view reconstruction techniques, while utilizing geometric relationships as indoor structure priors. Therefore, we describe existing work on the following three domains: 1) single-view techniques for 3D reconstruction, 2) multi-view reconstruction techniques, and 3) the use of structure priors for 3D reconstruction.

Single view technique: A careful analysis of lines, its connections, and its vanishing points has enabled a single-image reconstruction of architectural scenes [16, 15]. However, these algorithms critically depend on the connectivity of lines and can easily fail. For indoor scenes, a single image scene understanding has been a very active topic [8, 14, 34]. Similar work exists for outdoor scenes [6]. However, their 3D models are mostly a combination of boxes for the purpose of scene understanding rather than reconstruction. Superpixel and line analysis allows more complicated reconstruction of an indoor scene [32]. More recently, data driven approaches, in particular deep networks, have demonstrated interesting single-view reconstruction results [28, 12]. Despite being an exciting new direction, these reconstructions are rough and do not match up with the quality of multi-view reconstructions.

Multi-view technique: State-of-the-art SfM algorithms work very well for texture-rich scenes with reasonable baselines. In 2006, Snavely et al. introduced a powerful "Incremental SfM" algorithm [22], which incrementally grows SfM models. In 2011, Crandall et al. proposed a global approach, which seeks to estimate all the camera parameters simultaneously [3]. Currently, many state-of-the-art SfM or SLAM (Simultaneous Localization and Mapping) algo-

rithms follow this "global approach".

Shum and Szeliski in the nineties [20] or Richardt et al. more recently [17] have demonstrated panoramic 3D reconstruction from rotation-dominant motions. Yu et al. [33] or Ha et al. [7] succeeded in solving SfM from accidental camera motions. However, these methods assume rich texture and rely on visual feature tracking/matching with careful multi-view geometric analysis for 3D reconstruction. [1] Texture-less scenes with limited camera translations still pose major challenges for existing SfM algorithms.

Structure priors for 3D reconstruction: Structure priors have played an important role in the advancement of 3D Computer Vision. Flint et al. [5] has proposed an effective indoor scene reconstruction algorithm by assuming that an indoor scene consists of two horizontal surfaces and vertical walls. This type of high-level structural priors have also been the key to the success of single-view reconstruction techniques. However, in the domain of SfM or SLAM, only low-level geometric priors have been exploited in the past, often just lines and vanishing points [26, 9, 19, 4, 10] or planes at best [18]. In this paper, we seek to exploit a family of geometric relationships between lines to better constrain challenging reconstruction problems.

3. Input data

We have developed simple iOS and Android apps that record 360° panoramic videos and IMU rotations (See Fig. 2). Both iOS and Android offer an API to retrieve camera rotations after sensor fusion. Similar to Google Cardboard Camera App, we have recorded videos with a "natural" body motion in which the human body is at the center

---

[1] Google Cardboard Camera App produces stereoscopic panoramas from panoramic movies. Although its algorithmic details are not disclosed, feature tracking/matching is probably their primary geometric cues.
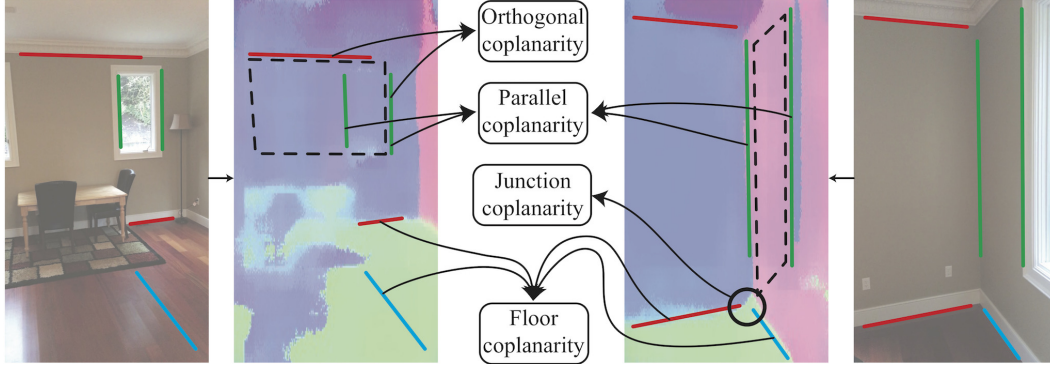
Figure 3. We identify four different types of coplanarity relationships among line segments by utilizing a surface normal estimate by a deep-network [28]. The colors of line segments represent their corresponding Manhattan directions.

of rotation, as opposed to an "unnatural" motion where the camera must be at the center of rotation. This camera motion ensures some amount of parallax, although being too small for standard SfM or SLAM algorithms. Our approach identifies geometric constraints to enable 3D reconstruction even from such small translational motions.

4. Panoramic Structure from Motion

The input to our pipeline is a panoramic image stream with initial camera rotations from the iOS or Andorid app as well as intrinsics from precalibration [2]. The pipeline consists of four steps: 1) preprocessing, 2) geometric relationship detection, 3) linear SfM, and 4) bundle adjustment. The second and third steps are the core of this paper. We now explain the details of each step.

4.1. Preprocessing

The goal of the preprocessing step is three-fold: Manhattan direction extraction, Manhattan line tracking, and camera rotation refinement. The procedure is based on standard techniques, and we here briefly describe the procedure, and refer some algorithmic and implementation details to the supplementary material.

Line segment detection: First, we use a standard line segment detection software (LSD [27]) to extract line segments from each input image. We use the existing algorithm [25] to merge neighboring line segments when their angle differences are less than 1 degree and the minimum distance between their endpoints is less than $0.05 \times min(w, h)$ pixels where (w, h) are the width and height of the input image, respectively. After the merging, we discard line segments that are shorter than $0.05 \times min(w, h)$ pixels.

Manhattan frame extraction: Given reasonable initial camera rotations and intrinsics, we extract the Manhattan frame from the detected lines in all the images: 1) We let each line cast votes to its potential 3D directions (i.e., a great circle) on a Gaussian sphere; then 2) sequentially ex-

tract Manhattan directions by detecting peaks while enforcing the mutual orthogonality.

Manhattan line extraction: We detect *Manhattan line segments* by simply collecting lines that cast votes to each of the three peaks within a certain margin (10 degrees on the voting sphere). We avoid detecting degenerate lines that are associated with two or more Manhattan directions.

Rotation refinement: Since initial rotations from IMU usually contain drifting errors, we use standard non-linear least squares optimization [1] to refine camera rotations so that the detected Manhattan line segments pass through the corresponding Manhattan vanishing points. We repeat the Manhattan axis extraction, Manhattan line extraction, and rotation refinement a few times.

Line tracking: Lastly, we form tracks of Manhattan line segments by grouping nearby line segments along the same Manhattan direction across frames.

4.2. Geometric relationship detection

Rough surface normal estimations suffice to extract powerful geometric constraints among lines. We first use a deep-network by Wang et al. [28] to obtain the surface normal estimation for each input image. Since estimated surface normals are defined on each camera coordinate frame, we project each normal onto the global Manhattan coordinate system using the rotation matrices.

Three types of coplanarity relationships are detected for every pair of line segments in each frame. The fourth coplanarity test finds and enforces line segments on the floor to be coplanar, providing precise geometric constraints across all the frames even without any visual overlap (See Fig. 3).

Orthogonal coplanarity: Our input is Manhattan lines, each of which is associated with one of the three Manhattan directions. Suppose one is given a pair of lines associated with different Manhattan directions. If the pair is coplanar, the space between these two lines should have the same surface normal pointing towards the orthogonal Manhattan
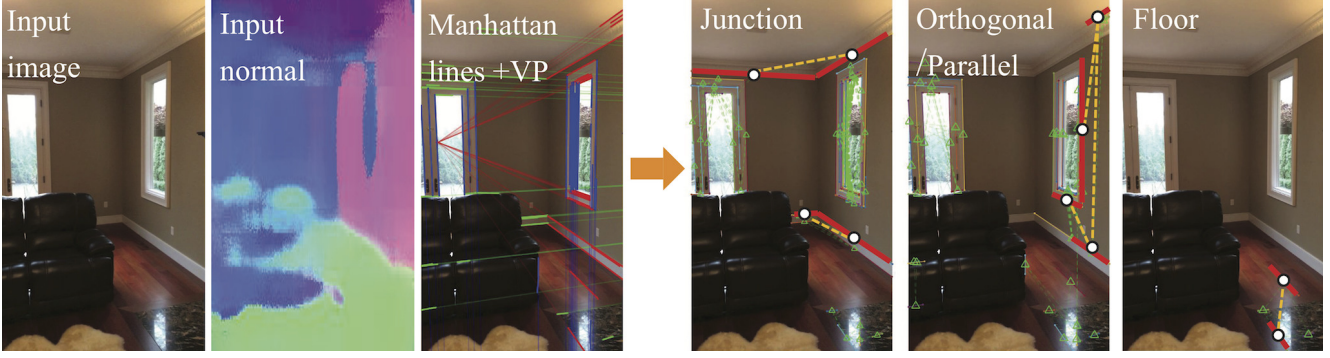
Figure 5. Geometric relationship detection. Given a video sequence and a set of normal images (1st and 2nd images), our framework estimates the Manhattan-world vanishing points and cluster each line segment into one of three three Manhattan axes (3rd image). Then, we detect four different types of coplanarity relationships among line segments: junction, orthogonal, parallel, or floor coplanarity. To avoid clutter, we only show a small number of detected geometric relationships.
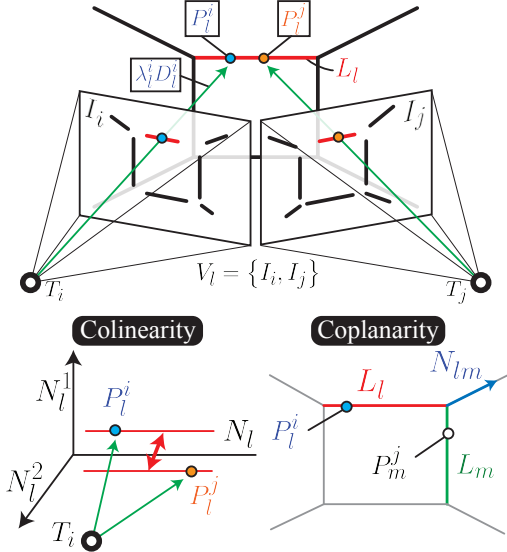

Figure 4. Linear SfM formulation with geometric constraints. Suppose a line L_l was detected and formed a track in images $V_l = \{I_i, I_j\}$. The mid-point (P_l^i) of a line segment in an image (I_i) is parameterized by the depth (λ_l^i). The line direction is a known Manhattan direction. We enforce detected coplanarities between a pair of lines as well as the colinearity between P_l^i and P_l^j.

direction. Therefore, we compute the average surface normal inside a quad defined by the four end-points of the line segments, then declare Manhattan coplanarity if the following two conditions are met: 1) the average normal is within $20°$ from the expected Manhattan direction and 2) the average angle difference between the average normal and all the surface normals inside the quad is less than $5°$.

Parallel coplanarity: Given a pair of lines with the same Manhattan direction, we detect the coplanarity in exactly the same way as in the Orthogonal coplanarity case with one difference. Parallel lines are always coplanar, and we restrict the potential coplanarity normal to be one of the

remaining two Manhattan directions. For instance, if two lines are parallel along the X-axis, the coplanarity normal must be either along Y or Z axis.

Junction coplanarity: Given a pair of lines with different Manhattan directions, two lines are deemed to be coplanar if their end-points are close, that is, within $0.1 \times min(h, w)$.

Floor coplanarity: The floor coplanarity segments the floor region in each frame by collecting pixels whose normals are within $25°$ degrees from the vertical direction. We apply a morphological operation (dilation) once then find line segments that are fully contained inside the floor regions. We enforce these lines from all the frames to be coplanar on a horizontal surface (i.e., floor). Notice that existing SfM/SLAM algorithms require features to be commonly visible across frames. The floor coplanarity is unusually powerful and can provide constraints among all the frames even when there are no visual overlap.

4.3. Linear SfM formulation

Sinha et al. proposed a linear SfM formulation that minimizes reprojection errors as linear functions of the point 3D coordinates and camera translations [21]. We have formulated a linear SfM problem that minimizes colinearity and coplanarity constraints among lines as linear functions of the line parameters and camera translations.

Model: IMU rotations and the camera intrinsics from the precalibration step allow us to focus on the estimation of camera translations ($\{T_i\}$) and the 3D model, in our case, 3D lines. Since we know the direction of a line (i.e., one of the Manhattan directions), estimating the depth of a single reference point on a line suffices to uniquely determine its geometry (See Fig. 4). In particular, we seek to estimate the depth λ_l^i of a tracked line at its mid-point P_l^i in each image, where i and l are the image and line indexes, respectively:

$$P_l^i = T^i + \lambda_l^i D_l^i.$$

D_l^i is the unit-length viewing ray for P_l^i. The depths are measured along the rays as opposed to along the optical axis of the image. Note that we estimate multiple depth values for a single line-track, making our line parameterization redundant. However, we have chosen this simple parameterization because the core solver (constrained linear least squares) is scalable. In the bundle adjustment step conducting non-linear optimization next, we will use more compact line parameterization. Unknown variables of our SfM problem are camera translations and line depths, subject to the following two linear constraints.

Colinearity constraints: A single line-track has multiple depth values estimated across tracked images. Lines must be reconstructed exactly at the same location, and we enforce colinearity among such lines. More precisely, give a line, for every pair of tracked images (I^i, I^j), we measure the distance between the two lines along their orthogonal Manhattan directions (N_l^1, N_l^2):

$$\left(P_l^i - P_l^j\right) \cdot N_l^1 = 0, \quad \left(P_l^i - P_l^j\right) \cdot N_l^2 = 0.$$

Coplanarity constraints: Let P_l^i and P_m^j be two lines that have been detected as coplanar. We impose coplanarity as

$$(P_l^i - P_m^j) \cdot N_{l,m} = 0.$$

$N_{l,m}$ is the surface normal of the detected plane.

These constraints are linear functions of the variables ($\{T_i\}$, $\{\lambda_l^i\}$). As λ (depth) must be positive, we add the non-negativity constraint for the depth variables, then use the standard dual active-set method in QPC [29].

4.4. Bundle adjustment

Bundle adjustment further improves the quality of 3D models and camera parameters. This time, we employ more compact line parameterization introduced in [26]. To be more specific, a line L_l is parameterized by a vector Λ_l that connects the origin and the closest point on the line. It is easy to show that Λ_l becomes perpendicular to the direction of a line. The residual again consists of the three terms.

Colinearity: Since Λ_l is perpendicular to the line direction, which we denote as A_l, their dot-product must be 0:

$$A_l \cdot \Lambda_l = 0.$$

Coplanarity: Given two lines that must be coplanar and are parameterized by Λ_l and Λ_m, respectively, the distance of the two lines along the coplanar normal direction (A_{lm}) must be 0:

$$(\Lambda_l - \Lambda_m) \cdot A_{lm} = 0.$$

Reprojection errors: We project a line L_l to all its tracked images and measure the reprojection errors against the line segments in the images. There are many ways to measure the line reprojection errors. We simply measure the average distance over all the points on the line segment to the projected line [26].

We use a standard non-linear least squares optimization library Ceres [1] to refine the parameters. The weights of the three residuals are set to 1 for the reprojection error and 10^4 for the colinearity and coplanarity errors. Following recent trends in SfM literature [13], we solve this bundle adjustment problem in three phases. In the first phase, we only refine line parameters and camera translations. We then add camera rotations in the second phase, and camera intrinsics in the last phase for refinement.

5. Experimental results

We have evaluated the proposed approach with five challenging datasets. The first four datasets have been captured in a residential house and named *Living room* (340 frames), *Bed room* (341 frames), *Play room* (296 frames), and *TV room* (294 frames). The resolution of these datasets are 1980×1080 (iPhone6s). The fifth dataset was captured at an atrium of a University building: *Atrium* (361 frames). The resolution of this dataset is 1280×800 (Nexus 9 tablet). All the datasets have been recorded as 30 fps videos, and subsampled so that $360°$ are covered by roughly 360 frames.

We have used a PC with an Intel Core i7-4770 (3.40GHz, single thread) processor and 32.0GB ram. MATLAB with some C++ mex functions have been used for the implementation. The rough processing times of our computationally expensive steps are 1) 30 seconds for the line detection and merging; 2) 1 minute for the vanishing point estimation and rotation refinement; 3) 2 minutes for the line tracking; 4) 5 seconds per image for the coplanarity estimation; 6) 30 seconds for solving a constrained linear least squares problem; and 7) 1 minute for the bundle adjustment.

The main experimental results are illustrated in Fig. 6. The proposed approach has successfully recovered near-complete 3D models, registering more than 90% of the frames in each dataset. Figure 7 illustrates the contributions of different geometric relationships, where we have run our algorithm on *Atrium* with three different sets of relationships: 1) junction coplanarity only; 2) junction, orthogonal, and parallel coplanarities; and 3) everything. In addition to making the 3D structure more accurate, the geometric relationships help connect more images and models, which would otherwise be disconnected and become scale-ambiguous, the major and most problematic failure modes of current SfM methods.

We have compared against a wide range of SfM (SLAM) software to assess challenges in our panoramic movie datasets. First, Figure 8 shows the reconstruction results of the four state-of-the-art SfM/SLAM systems with ours

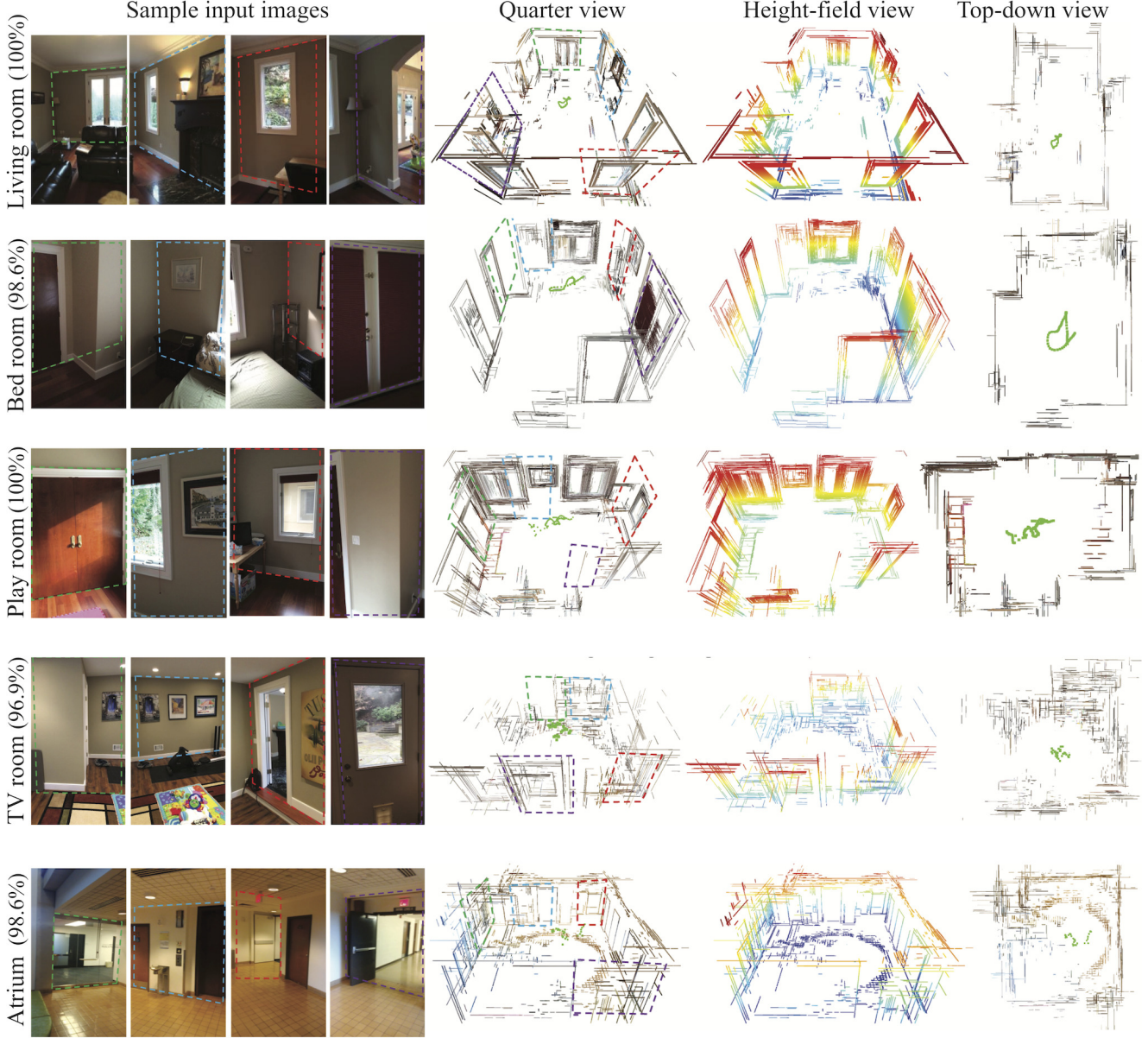| | Sample input images | Quarter view | Height-field view | Top-down view |

Figure 6. Sample input images and our line models in three different views. The quarter view renders each line with its average color in the images. The height-field view uses the heat-map color scheme based on the heights from the floor. The top-down view is an orthographic projection view from the top. Recovered camera centers are shown by green dots. The numbers show the ratios of registered frames.

for Play room, which is a relatively easier dataset with rich textures. The left two methods are so-called "Incremental SfM", which sequentially adds cameras and grows the model. The next two methods are "Global SfM", which simultaneously recovers all the camera parameters. For fairness, camera intrinsics have been provided to each software as either initialization or fixed parameters, except that we could not figure out a way to specify in Theia. As the figure illustrates, Global SfM is the state-of-the-art approach and outperforms in this challenging example. We have also tried to evaluate small-motion SfM algorithms, in particular,

DfUSMC by Ha et al. [7]. However, they could not produce any models as the software assumes that feature tracks must be fully visible throughout the video. In rotation-heavy panoramic movies, features quickly go outside frames and tracks become short, another challenge in our problem.

To further evaluate the effectiveness of our method, Figure 9 shows the reconstructed models of OpenMVG [13], the best method in the previous experiment, on all the datasets. In addition to the intrinsics (the top row), we have also provided the IMU camera rotations as the initialization (the bottom row). The ratios of registered frames sug-
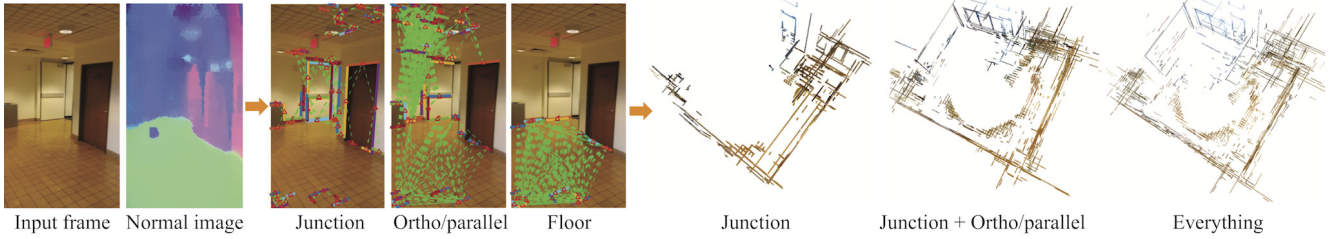
Figure 7. Contributions of the four coplanarity relationships, detected in the *Atrium* dataset. We have run our reconstruction algorithm with three different sets of coplanarity relationships: 1) junction coplanarity only; 2) junction, orthogonal, and parallel coplanarities; and 3) all the four. The middle shows the pairs of line segments detected as coplanar.

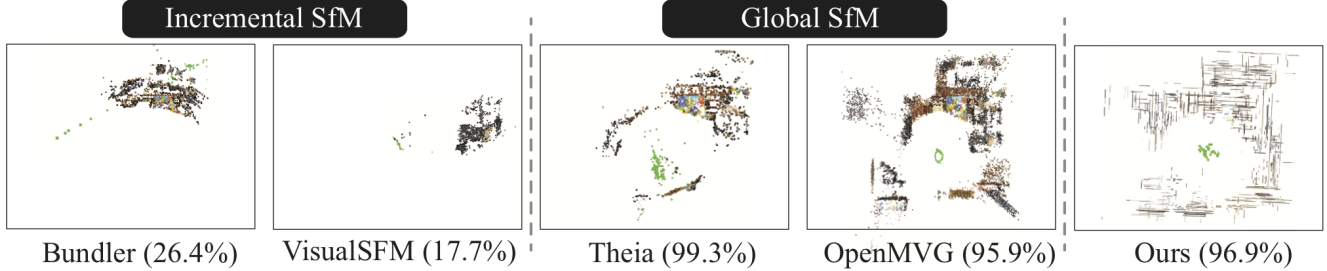Bundler (26.4%)   VisualSFM (17.7%)   Theia (99.3%)   OpenMVG (95.9%)   Ours (96.9%)

Figure 8. Comparison against state-of-the-art SfM (SLAM) systems, Bundler [22], VisualSFM [30], Theia [23], and OpenMVG [13] for TV room. Each number shows the ratio of registered frames. Only OpenMVG and our approach have produced near perfect models.

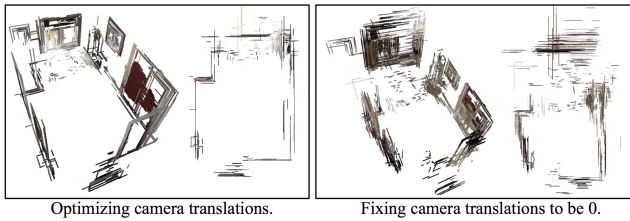Optimizing camera translations.   Fixing camera translations to be 0.

Figure 11. Estimation of the camera translation in the SfM framework is crucial in obtaining a clean model.

gest that OpenMVG has produced near complete models for most of the examples. However, the effective completeness of the OpenMVG models appear much lower, especially in the left three examples, where scarce features and small translations pose challenges.

A quantitative evaluation of scene reconstructions with a ground-truth is a challenging task especially for complex indoor environments. We have manually clicked correspondences across multiple images, triangulated the 3D point, and used its reprojection errors as the accuracy measure (See Fig. 10). More precisely, for each dataset, we have selected six images with some visual overlap, where OpenMVG has estimated camera parameters. The table shows the means and standard deviations of the reprojection errors in pixels. Note that the resolution of the input images are 1980×1080 except for the Atrium dataset whose resolution is 1280×800. Our indoor panoramic image streams are extremely challenging as distinctive visual feature points are

often rare in a sequence, and reprojection errors are relatively large throughout the sequences. Nonetheless, our errors are often a few times smaller than those of OpenMVG.

Our final experiment is to verify the importance of camera translation estimation in the SfM framework. We have simply run our algorithm while enforcing camera translations to be 0, which resembles a problem setting for line-based single view reconstruction. Figure 11 shows that the translation estimation is crucial in obtaining a clean 3D model without corruption. Please also see the supplementary video for the full assessment of the input videos and the reconstruction results.

6. Conclusions

This paper tackles a challenging panoramic SfM problem, where input images have minimal parallax and lack in rich visual textures. Our approach detects coplanarity relationships between pairs of lines by utilizing a deep-network for the surface normal estimation. The detected relationships provide exact geometric constraints in solving a line-based SfM problem. The presented method has outperformed many state-of-the-art SfM (SLAM) algorithms on our challenging datasets. The current limitation of our approach is the false coplanarity detection. While 3D structure looks clean, reprojection errors are still too large to run a stereo algorithm for obtaining a dense geometry. Our future work is to 1) incorporate point features into the framework; 2) train a proper relationship classification machinery given an image and a pair of lines; and 3) develop robust opti-
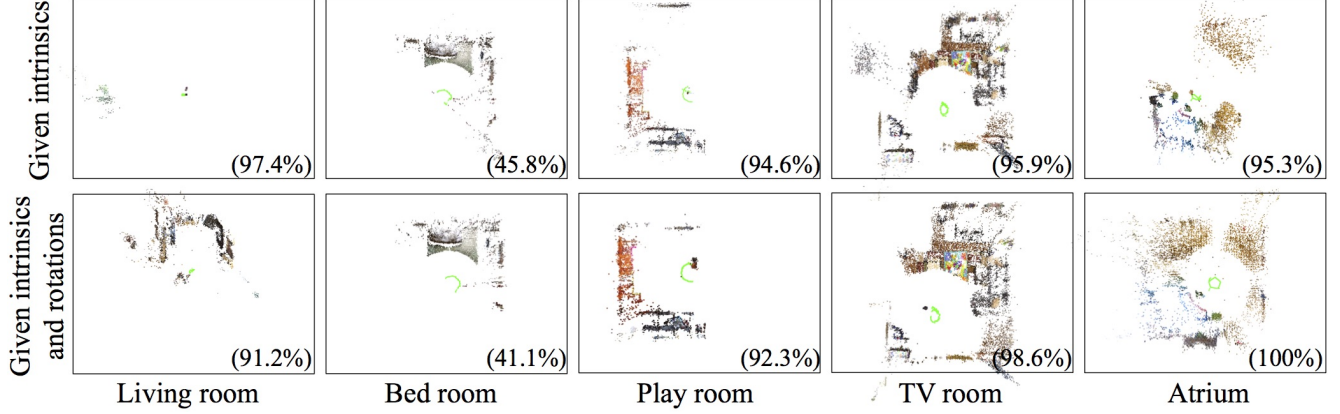
Figure 9. OpenMVG results in a top-down view. For being fair, the intrinsics are initialized to the values in our pre-calibration process in the top row. Both the intrinsics and camera rotations are initialized in the bottom row. The numbers show the ratios of registered frames.

□ Manual matches   + Ours (Before BA)   + Ours (After BA)   + OpenMVG

	Mean reprojection errors (px)					Standard deviations (px)				
	Living room	Bed room	Play room	TV room	Atrium	Living room	Bed room	Play room	TV room	Atrium
Ours (Before BA)	91.6	127.3	174.6	113.5	114.1	38.5	64.2	114.3	93.8	105.2
Ours (After BA)	40.2	95.5	131.6	44.6	46.6	36.5	95.0	64.0	15.8	34.1
OpenMVG	64.1	230.4	302.7	34.0	70.4	26.2	75.5	145.8	27.6	35.5

Figure 10. Reprojection error analysis in the *Living room* (left) and *Bed room* (right) datasets. We have triangulated a 3D point from manual correspondences (yellow rectangles), then plot reprojected pixel coordinates based on the camera parameters of our method (before or after the bundle adjustment) and OpenMVG. The table shows the means and standard deviations of the reprojection errors in pixels.

mization strategy to handle outliers.

References

[1] S. Agarwal, K. Mierle, and Others. Ceres solver. http://ceres-solver.org. 3, 5

[2] J.-Y. Bouguet. Camera calibration toolbox for matlab. http://www.vision.caltech.edu/bouguetj/calib_doc/. 3

[3] D. Crandall, A. Owens, N. Snavely, and D. Huttenlocher. Discrete-continuous optimization for large-scale structure from motion. In CVPR, pages 3001–3008. IEEE, 2011. 2

[4] A. Elqursh and A. Elgammal. Line-based relative pose estimation. In CVPR, pages 3049–3056. IEEE, 2011. 2

[5] A. Flint, C. Mei, D. Murray, and I. Reid. A dynamic programming approach to reconstructing building interiors. In ECCV, pages 394–407. 2010. 2

[6] A. Gupta, A. A. Efros, and M. Hebert. Blocks world revisited: Image understanding using qualitative geometry and mechanics. In ECCV, pages 482–496, 2010. 2

[7] H. Ha, S. Im, J. Park, H.-G. Jeon, and I. So Kweon. High-quality depth from uncalibrated small motion clip. In Proceedings of the IEEE Conference on Computer Vision and Pattern Recognition, pages 5413–5421, 2016. 2, 6

[8] V. Hedau, D. Hoiem, and D. Forsyth. Recovering the spatial layout of cluttered rooms. In ICCV, pages 1849–1856, 2009. 2

[9] W. Y. Jeong and K. M. Lee. Visual SLAM with line and corner features. In Intelligent Robots and Systems, IEEE/RSJ International Conference on, pages 2570–2575. IEEE, 2006. 2

[10] C. Kim and R. Manduchi. Planar structures from line correspondences in a Manhattan world. In ACCV, pages 509–524, 2014. 2

[11] F. Liu, C. Shen, and G. Lin. Deep convolutional neural fields for depth estimation from a single image. In CVPR, pages 5162–5170, 2015. 1

[12] A. Mallya and S. Lazebnik. Learning informative edge maps for indoor scene layout prediction. In ICCV, pages 936–944, 2015. 2

[13] P. Moulon, P. Monasse, R. Marlet, and Others. OpenMVG. An open multiple view geometry library. https://github.com/openMVG/openMVG. 5, 6, 7

[14] P. K. Nathan Silberman, Derek Hoiem and R. Fergus. Indoor segmentation and support inference from RGBD images. In ECCV, 2012. 2

[15] S. Ramalingam and M. Brand. Lifting 3D manhattan lines from a single image. In ICCV, pages 497–504, 2013. 2

[16] S. Ramalingam, J. Pillai, A. Jain, and Y. Taguchi. Manhattan junction catalogue for spatial reasoning of indoor scenes. In CVPR, pages 3065–3072, 2013. 1, 2

[17] C. Richardt, Y. Pritch, H. Zimmer, and A. Sorkine-Hornung. Megastereo: Constructing high-resolution stereo panoramas. In CVPR, pages 1256–1263, 2013. 1, 2

[18] R. F. Salas-Moreno, B. Glocken, P. H. Kelly, and A. J. Davison. Dense planar SLAM. In ISMAR, pages 157–164. IEEE, 2014. 2

[19] G. Schindler, P. Krishnamurthy, and F. Dellaert. Line-based structure from motion for urban environments. In 3D Data Processing, Visualization, and Transmission, Third International Symposium on, pages 846–853. IEEE, 2006. 2

[20] H.-Y. Shum and R. Szeliski. Stereo reconstruction from multiperspective panoramas. In ICCV, 1999. 2

[21] S. N. Sinha, D. Steedly, and R. Szeliski. A multi-stage linear approach to structure from motion. In ECCV Workshop on Reconstruction and Modeling of Large-Scale 3D Virtual Environments, 2010. 4

[22] N. Snavely, S. M. Seitz, and R. Szeliski. Photo Tourism: Exploring image collections in 3d. In SIGGRAPH, 2006. 2, 7

[23] C. Sweeney. Theia multiview geometry library: Tutorial & reference. University of California Santa Barbara, 2, 2015. 7

[24] R. Szeliski. Computer Vision: Algorithms and Applications. Springer, 2010. 1

[25] J. M. R. S. Tavares and A. J. M. N. Padilha. A new approach for merging edge line segments. RecPad95, 1995. 3

[26] C. J. Taylor and D. J. Kriegman. Structure and motion from line segments in multiple images. TPAMI, 17(11):1021–1032, 1995. 2, 5

[27] R. G. von Gioi, J. Jakubowicz, J.-M. Morel, and G. Randall. LSD: A fast line segment detector with a false detection control. TPAMI, (4):722–732, 2008. 3

[28] X. Wang, D. Fouhey, and A. Gupta. Designing deep networks for surface normal estimation. In CVPR, pages 539–547, 2015. 1, 2, 3

[29] A. Wills. QPC - quadratic programming in c. http://sigpromu.org/quadprog/. 5

[30] C. Wu. VisualSFM : A visual structure from motion system. http://ccwu.me/vsfm/. 7

[31] J. Xiao, A. Owens, and A. Torralba. SUN3D: A database of big spaces reconstructed using SfM and object labels. In ICCV, pages 1625–1632, 2013. 1

[32] H. Yang and H. Zhang. Efficient 3d room shape recovery from a single panorama. In Proceedings of the IEEE Conference on Computer Vision and Pattern Recognition, pages 5422–5430, 2016. 2

[33] F. Yu and D. Gallup. 3D reconstruction from accidental motion. In CVPR, pages 3986–3993, 2014. 2

[34] Y. Zhang, S. Song, P. Tan, and J. Xiao. PanoContext: A whole-room 3d context model for panoramic scene understanding. In ECCV, pages 668–686, 2014. 1, 2

Panoramic Structure from Motion via Geometric Relationship Classification
Supplementary material

Satoshi Ikehata and Yasutaka Furukawa
Washington University in St. Louis

Ivaylo Boyadzhiev and Qi Shan
Zillow

The supplementary material provides algorithmic and implementation details of the three preprocessing steps: (1) Manhattan frame (direction) extraction, (2) camera rotation refinement, and (3) Manhattan line tracking. These steps rely on standard techniques and are described here.

1. Manhattan frame extraction

Manhattan frame extraction aims to recover the three orthogonal Manhattan directions given images, camera intrinsics and IMU rotation matrices.

We follow the VP representation as in [3]. The 3D vanishing directions are represented by the intersections of multiple *interpretation planes*. A interpretation plane is spanned by the global origin and the two unit vectors that pass both the origin and endpoints of each line segment in the global space. A homogeneous point vector $\tilde{\mathbf{x}}$ on the i-th image is computed by $R_i^T K^{-1} \tilde{\mathbf{x}}$ where K and R_i are the camera intrinsic matrix and the i-th IMU rotation matrix, respectively.

To extract Manhattan frames, we first uniformly discretize the Gaussian sphere centerd on the optical center of the camera into 10242 directions [4], and project the interpretation plane of each line segment to the Gaussian sphere using camera information. Let $w \in \mathcal{R}^+$ be the length of a line segment on the image. We accumulate w votes to the discretized bin when the angle difference between the interpretation plane and the vector on the Gaussian sphere is less than 0.03 in radius. Finally, we normalize the voting map by the maximum value over all the bins to acquire the normalized Gaussian sphere. Figure 1 shows one example.

The Manhattan frames are extracted by using the votes on the Gaussian sphere. We use a simple peak extraction algorithm as follow. First, we find the maximum peak that is near from the gravity direction given by the IMU sensor ($\mathbf{v}_z$). Then, we subsample the vectors on the Gaussian sphere whose angle differences between the peaks and the vector are less than one degree. From this subset, we find the second peak that has the maximum votes ($\mathbf{v}_x$) and the third vector ($\mathbf{v}_y$) that is orthogonal to both $\mathbf{v}_x$ and $\mathbf{v}_z$.

We should note that the extracted vanishing directions may contain errors. The next step improves these vanishing

directions as well as the camera rotation matrices:

2. Rotation refinement

The global rotation matrices given by the IMU in the consumer smartphones contain non-negligible errors. Therefore, we refine rotation matrices using extracted Manhattan frames.

In each image, we declare a line segment as a *Manhattan line segment* if the angle difference between the normal of the interpretation plane and one Manhattan direction is more than 85 degrees, and the same angle difference with the other two Manhattan directions are both less than 85 degrees. The second condition is critical to avoid ambiguous line segments that correspond to two Manhattan directions. Given m images and $N(i)$ Manhattan line segments, we refine rotation matrices by minimizing the following functional:

$$\sum_{i=1}^{m} \sum_{j=1}^{N(i)} \left| \frac{(R_i^T K^{-1} \tilde{\mathbf{p}}_{i,j} \times R_i^T K^{-1} \tilde{\mathbf{q}}_{i,j})^T}{|R_i^T K^{-1} \tilde{\mathbf{p}}_{i,j} \times R_i^T K^{-1} \tilde{\mathbf{q}}_{i,j}|} \mathbf{v}_{i,j} \right|_2^2$$
$$+ \lambda \sum_{(i,j) \in \mathcal{N}} \left| R_i^T R_j - R_i^{0T} R_j^0 u \right|_2^2. \quad (1)$$

$K \in \mathcal{R}^{3 \times 3}$ is the intrinsic camera matrix, and $R_i \in \mathcal{R}^{3 \times 3}$ and $R_i^0 \in \mathcal{R}^{3 \times 3}$ are the resulting and initial rotation matrices, respectively. $\tilde{\mathbf{p}}_{i,j} \in \mathcal{R}^{3 \times 1}$, $\tilde{\mathbf{q}}_{i,j} \in \mathcal{R}^{3 \times 1}$ and $\mathbf{v}_{i,j} \in \mathcal{R}^{3 \times 1}$ are homogeneous vectors of two endpoints and its vanishing direction of j-th Manhattan line segment on the i-th image, respectively. λ (set by 0.1 in our implementation) is a trade-off parameter between the data term and the smoothness term, respectively.

The first term penalizes the angular difference between the surface normal direction of the interpretation plane and the assigned vanishing direction. The second term seeks to make the relative rotation between nearby frames unchanged during the optimization. The term exploits the fact that IMU rotation may exhibit long-term accumulation errors, but are fairly accurate locally. $\mathcal{N}$ is constructed by the similarity of the z-axis of the camera coordinate frame that is corresponding to the display face direction of the de-
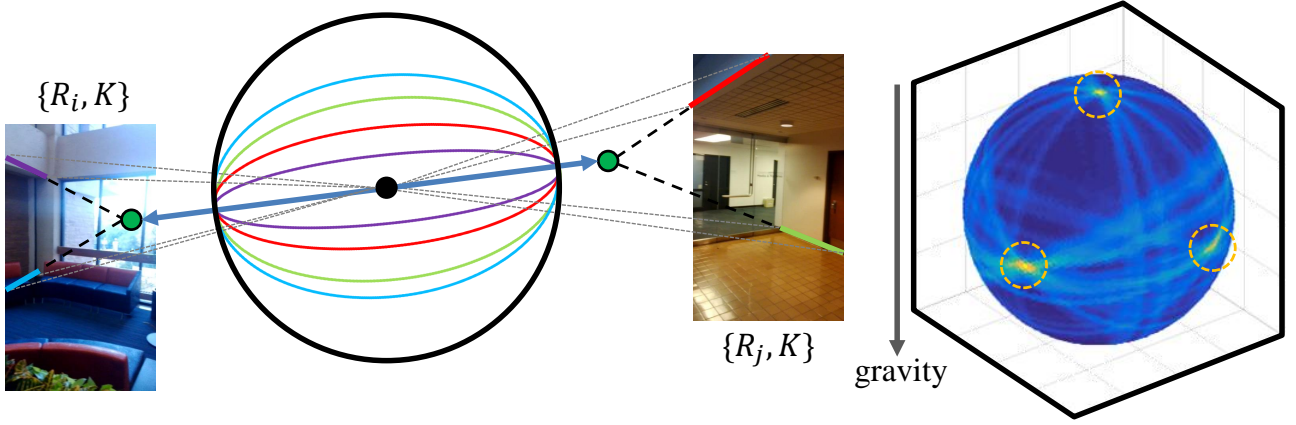
Figure 1. Manhattan frame extraction. (left) We vote along the interpretation plane on the Gaussian sphere. (right) vanishing directions are extracted at the peaks on the sphere.
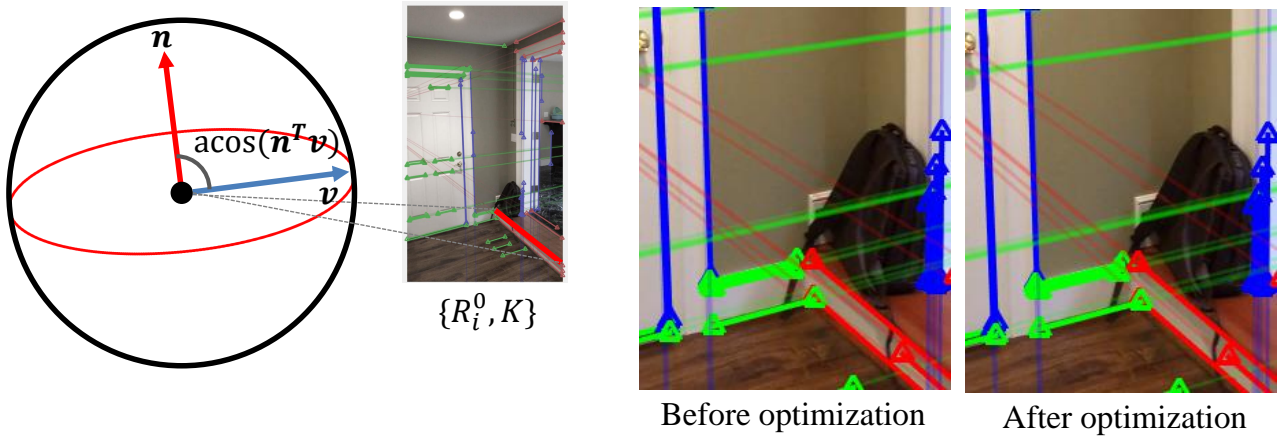

Figure 2. Rotation refinement. We iteratively update the rotations and Manhattan line segments until convergence.

vice. If the angle difference of the z-axes is less than 10 degrees, two cameras are considered as neighbors. Note that we repeat the process of extracting Manhattan line segments and optimizing Eq.1 until convergence (generally three iterations). Figure 2 shows that the Manhattan line segments and vanishing directions are refined over the iterations.

3. Line tracking

We match Manhattan line segments between pairs of frames, then find tracks. When the camera motion is purely panoramic, images are related by the Homography H [2] as

$$\tilde{x}_2 = H\tilde{x}_1, \qquad (2)$$

where $\tilde{x}_1$ and $\tilde{x}_2$ are the point location in the homogeneous coordinate. Since our input is panoramic videos, Eq. 2 is roughly satisfied. We find line tracks as follows.

First, we collect all the image pairs whose angle differences of the camera Z-axes are less than 2 degrees. For each

pair of images, a homography matrix H [2] is computed from SURF matches [1].

Suppose we seek to match a Manhattan line segment in one frame against a Manhattan line segment in another. We compute their distance as follows. First, we use the estimated Homography to warp one line segment to the other frame. Second, for each end-point of a line segment, compute the distance to a line containing the other line segment. 4 such distances are computed and we take the minimum as the distance between the two line segments. We declare that a pair of line segments match if 1) this distance is less than $0.05 \min(h, w)$; 2) the angle difference is less than 1 degree; and 3) they are mutually the closest line segment.

References

[1] H. Bay, T. Tuytelaars, and L. Van Gool. Surf: Speeded up robust features. In Computer vision–ECCV 2006,

pages 404–417. Springer, 2006. 2

[2] R. Hartley and A. Zisserman. Multiple view geometry in computer vision. Cambridge university press, 2003. 2

[3] T. Kroeger, D. Dai, and L. Van Gool. Joint vanishing point extraction and tracking. In Proceedings of the IEEE Conference on Computer Vision and Pattern Recognition, pages 2449–2457, 2015. 1

[4] J. Xiao, T. Fang, P. Zhao, M. Lhuillier, and L. Quan. Image-based street-side city modeling. In TOG, volume 28, page 114, 2009. 1